

# **Team SMOLDER HASP 2019 Final Science Report**

## **Multispectral Remote Sensing Study of Vegetation Indices By Dual Camera Imaging From A High Altitude Student Platform**

**Paras Angell, Megan Bromley, Henry Cardamone, David Lewis,  
Tim McMillen, Michael Oals, and Jenna Robinson**

Team SMOLDER Capstone HASP Project Report

School of Earth and Space Exploration

Arizona State University, Tempe

December 2019

## Table of Contents

Abstract.....	3
Introduction.....	4
Description of Payload.....	5
Results and Image Analysis .....	6
Discussion.....	22
Conclusions.....	25
Acknowledgements.....	27
References.....	27
Team Demographics .....	28
Team Graduation Information.....	29
Appendix A.....	30
Appendix B.....	31

## Abstract

Vegetation indices such as the Normalized Difference Vegetation Index (NDVI) are used to measure plant health from remote sensing images. Plant health can be an indicator of drought conditions and possible fire risk. NDVI is calculated from a ratio of differences of reflectivity of near infrared (NIR) and red light from a scene. Therefore multispectral imaging that includes red and NIR bands is used for evaluating NDVI which can be correlated to the presence of vegetation. The SMOLDER mission, which flew as a payload on the 2019 HASP, utilized two webcams with red and NIR filters (650 nm and 850 nm band centers respectively) in order to capture pairs of images to be used for post-flight NDVI calculations. The HASP balloon was successfully launched from Fort Sumner, New Mexico on September 5th, 2019 and flew towards Utah at a float altitude of ~36,000 meters. The flight lasted over 7 hours. The two SMOLDER webcams captured over 4,000 images along the 378 mile flight path. Lack of manual exposure control over the cameras led to overexposure “saturation” of most of the red band images. Therefore post-processing included selection of a regions of only the non-saturated pixels of each image pair. Although exposure time calibration could not be performed with the webcams, bandwidth ratio of 3.2 (80 nm bandwidth of red filter over 25 nm bandwidth of NIR filter) adjustment was performed prior to NDVI calculations. NDVI histograms, grayscale NDVI images, and false color NDVI images were produced and analyzed for image pairs along the flight path using davinci software. NDVI has a range of -1.0 to +1.0 with healthy plants yielding positive NDVI values. Most of the NDVI values observed in this study range from -0.8 to 0.0, with a few images showing NDVI values as high as +0.2, indicating that the terrain along the flight path does not contain significant vegetation. This mission was a success in demonstrating that multispectral remote sensing images can be obtained by a HASP payload and these images can be used to calculate vegetation indices.

## **1. Introduction**

The original science objective of this project is to investigate plant health by in-flight remote sensing imagery and correlate it to the presence of vegetation and desert rainfall. The science questions will address whether vegetation indices can be used as a proxy for determining desert drought conditions and understand how well vegetation indices correlate to desert rainfall.

SMOLDER stands for Small Mounted Optical Lenses Dual-camera Experimental Remote-sensor. SMOLDER was designed to be flown as a payload onboard the High Altitude Student Platform (HASP) balloon mission which is funded by NASA and hosted by Louisiana State University (LSU). The projected design of this payload was to carry two monochrome digital cameras pointed at the ground that will simultaneously record images of the scenery on the ground at two preselected wavelength bands. As the payload does not produce its own lighting to illuminate the scene being photographed, this project uses reflectance spectroscopy techniques to measure sunlight reflected off the surface features. The science objectives of this project are described in the following sections.

### **1.1 Remote Sensing Reflectance Spectroscopy**

When sunlight strikes objects, certain wavelengths of light are absorbed and other wavelengths are reflected. Different kinds of rocks and vegetation absorb and reflect different wavelengths. The reflectance of various wavelengths of light can be used to characterize materials such as rocks and plants. Many remote sensing studies have determined the reflectance spectra of healthy vegetation, unhealthy vegetation, soil, and other surface materials. Many satellite imaging systems such as USGS's Landsat series of systems utilize the characteristics of the reflectance spectra of surface materials. Materials reflect strongly or weakly in ultraviolet, blue, green, red, near infrared, or mid-infrared wavelengths. Healthy plants reflect strongly in near-infrared wavelengths around 850 nanometers (nm) and reflect weakly in red wavelengths around 650 nm.

## 1.2 Vegetation Indices

Therefore, the band ratio of near infrared (NIR) reflectance divided by reflectance in red can be used as a basic vegetation index (VI) [1-4]. More effective than a simple near IR to red band ratio is an index called NDVI [1,2]. NDVI stands for Normalized Difference Vegetation Index, and is given by the formula:

$$\text{NDVI} = \frac{(\rho_{\text{NIR}} - \rho_{\text{Red}})}{(\rho_{\text{NIR}} + \rho_{\text{Red}})} \quad (\text{Equation 1})$$

where rho ( $\rho$ ) indicates the reflectance from the scene at a specific wavelength.

NDVI can range from negative one to positive one. Vegetation appears dark in the visible wavelengths and bright in the near infrared. Typical NDVI values for brown leaves are close to zero, while NDVI values for green leaves are closer to one. NDVI is a measure of the density of plant growth. Very low values of NDVI (0.1 and below) correspond to barren areas of rock, sand, or snow. Moderate values represent shrub and grassland (0.2 to 0.3). High values indicate temperate and tropical rainforests (0.6 to 0.8) ([Earthobservatory.nasa.gov](http://Earthobservatory.nasa.gov)).

The primary objective of this project is to assess NDVI values from multispectral remote sensing images recorded during flight of the HASP Balloon and correlated to the presence of green vegetation along the flight path.

## 2. Description of Payload

Team SMOLDER payload consisted of two webcams controlled by a Raspberry Pi 3 Model B+ microcontroller. An Edmund optics red filter (650 nm center, 80 nm width) was placed in front of webcam A, and an Edmund optics near infrared filter (850 nm center, 25 nm width) was placed in front of webcam B. The controller, cameras, and filters were housed in an aluminum box with external power and communications connections to the HASP platform. A photograph of the payload is shown in Appendix A.

The inflight digital recording of the NIR and Red images was controlled by a Raspberry Pi that served as the onboard computer in the payload. The Raspberry Pi module was connected to two webcam cameras, one for the NIR wavelength band and another for the Red wavelength band. Raspberry Pi cameras were tested for this task, and monochrome USB cameras were tested as well. It is essential that either kind of camera does not have an infrared filter built into the camera. For taking the Red images, a Red filter is placed in front of the lens of that camera. This filter allows only Red wavelengths from 700 nm to 760 nm to pass into the camera. For taking the NIR images, a NIR filter is placed in front of the lens of the other camera so that camera receives light of wavelengths of 850 nm to 875 nm. Software programmed into the Raspberry Pi onboard computer recorded pairs of images at regular intervals. Each pair of images, one NIR, one Red, were stored on the SD card storage media plugged into the Raspberry Pi.

### **3 Results and Image Analysis**

#### **3.1 Data Collection Strategy**

The two webcams one with a red filter and the other with an infrared filter were connected to a Raspberry Pi system. The system was programmed to record an image with each camera using auto exposure setting which is the only exposure setting on a webcam. The pi was programmed to record one image with each camera in quick succession which was expected to yield a close approximation to taking simultaneous images with each camera. However, once an image was captured, a finite amount of time (3s to 5s) is required to write the image onto the Raspberry Pi SD card. Therefore, although the image pairs were recorded immediately after one another, they turned out to be 3 to 5 s apart. The images recorded by each camera were stored in a separate folder on the Raspberry Pi SD card. Over the 7 hour period of the HASP flight, about 2000 images were recorded by each camera.


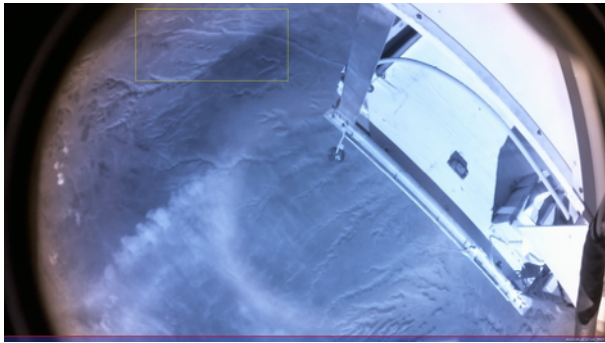
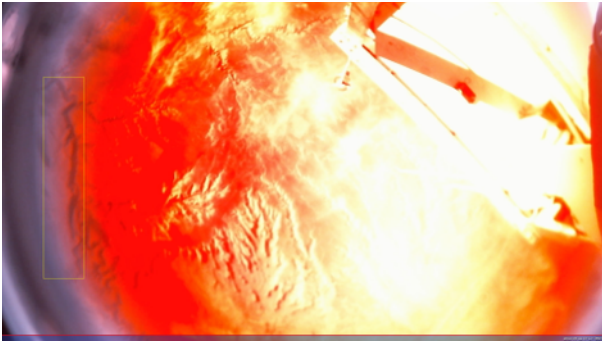
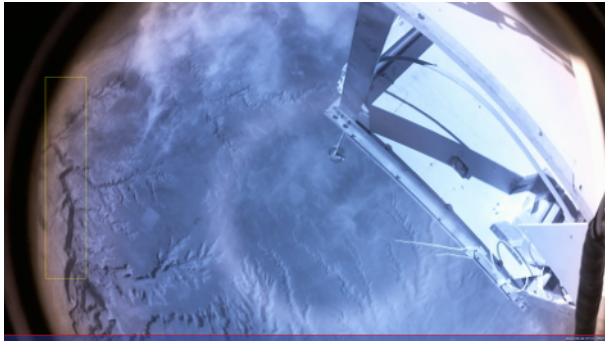
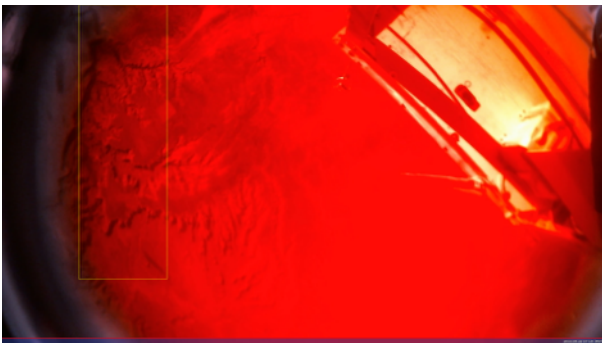
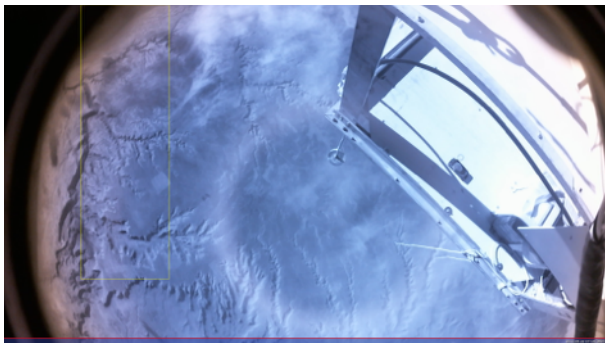
#### **3.2 Post Flight Data Processing**

Post-flight processing was performed on the images that had been captured during the HASP flight. The flight-SD card was retrieved from the payload and inserted it into another Raspberry Pi in the lab. From there the images were copied from the flight SD card to a jump drive which

was then used to transfer the images to another computer for analysis. A problem was encountered where the images could not be copied using either the Raspbian File Manager or the bash shell. The problem was due to the image files having colons in the file names. All attempts to copy the files resulted in a permissions error, however the issue was the colon characters in the file names, not actually file permissions. To work around this problem a script was written to copy each file and remove the colons from the time stamp part of the file name. For example, if the original file name on the payload was 2019-08-22 06:18:19.RAW, this was copied to the flash drive with a new name of 2019-08-22-061819.RAW.

### **3.3 Image Analysis**

When the images were first viewed, one set of images looked red and the other set looks blue. The red images were taken with the camera with webcam A which was covered with the red filter. The blue images were taken with webcam B with the Near IR filter. Most of the red images appear to be saturated, i.e. many regions of the red images were completely red and showed no detail. Three example pairs of images are shown in Figure 1. Each image pair has a red image and a near-infrared (NIR) image.

Example RAW Images	Example NIR Images
	
original Red image of image pair 061007 (all three bands)	original NIR image of image pair 061007 (all three bands)
	
original Red image of image pair 061725 (all three bands)	original NIR image of image pair 061725 (all three bands)
	
original Red image of image pair 061819 (all three bands)	original NIR image of image pair 061819 (all three bands)
Figure 1. Three pairs of raw unprocessed images from the two cameras. One camera had a red filter while the other had a near infrared (NIR) filter.	



To determine the degree of saturation, histograms were run on each of the bands of the red and NIR images for several pairs. Figure 2 shows a red image and three histograms which correspond to the red, green, and blue bands. It can be seen from the histogram (figure 2b) that most of the red band pixels have DN values greater than 250, which indicates overexposure/saturation in the red band.

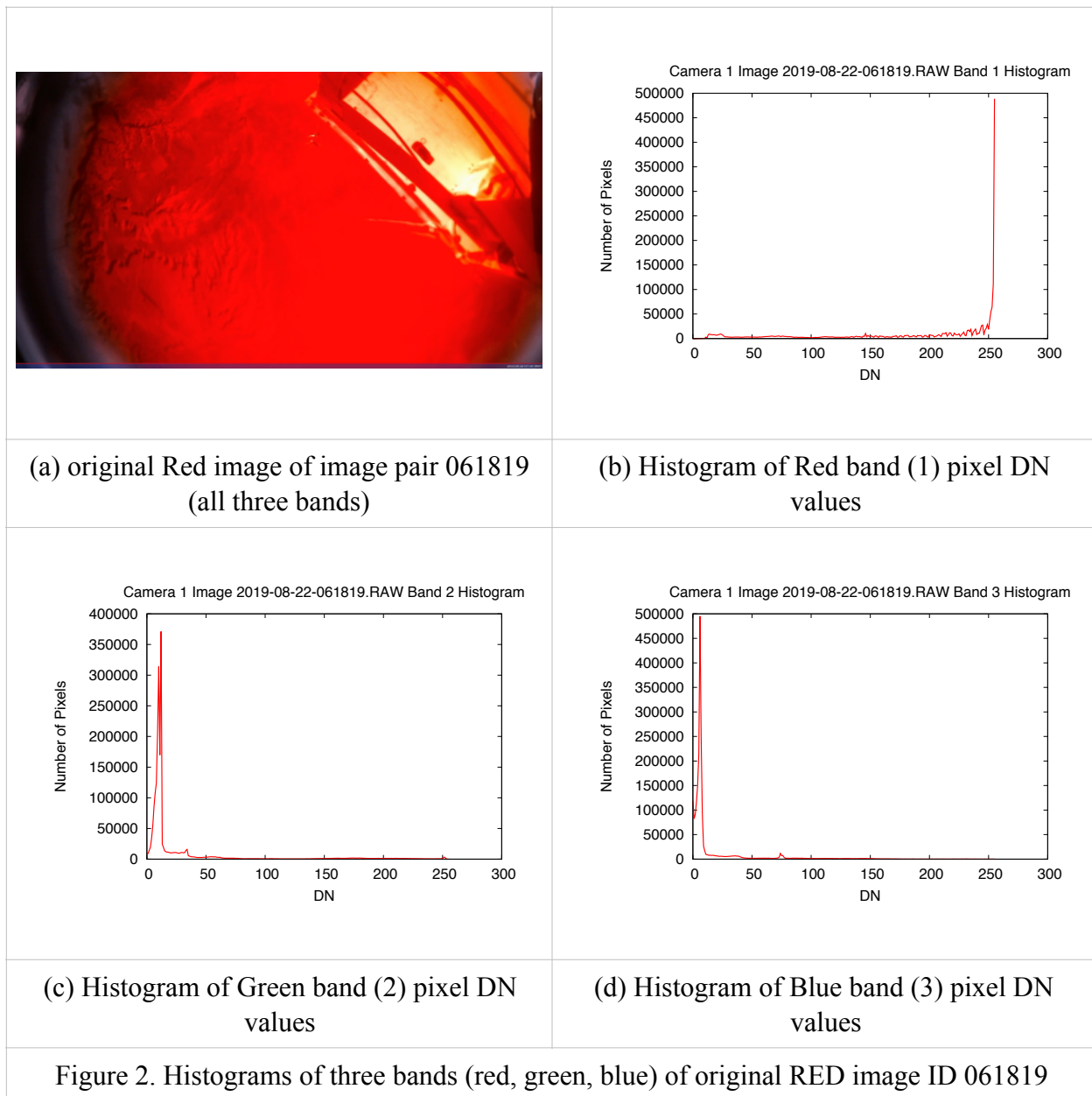
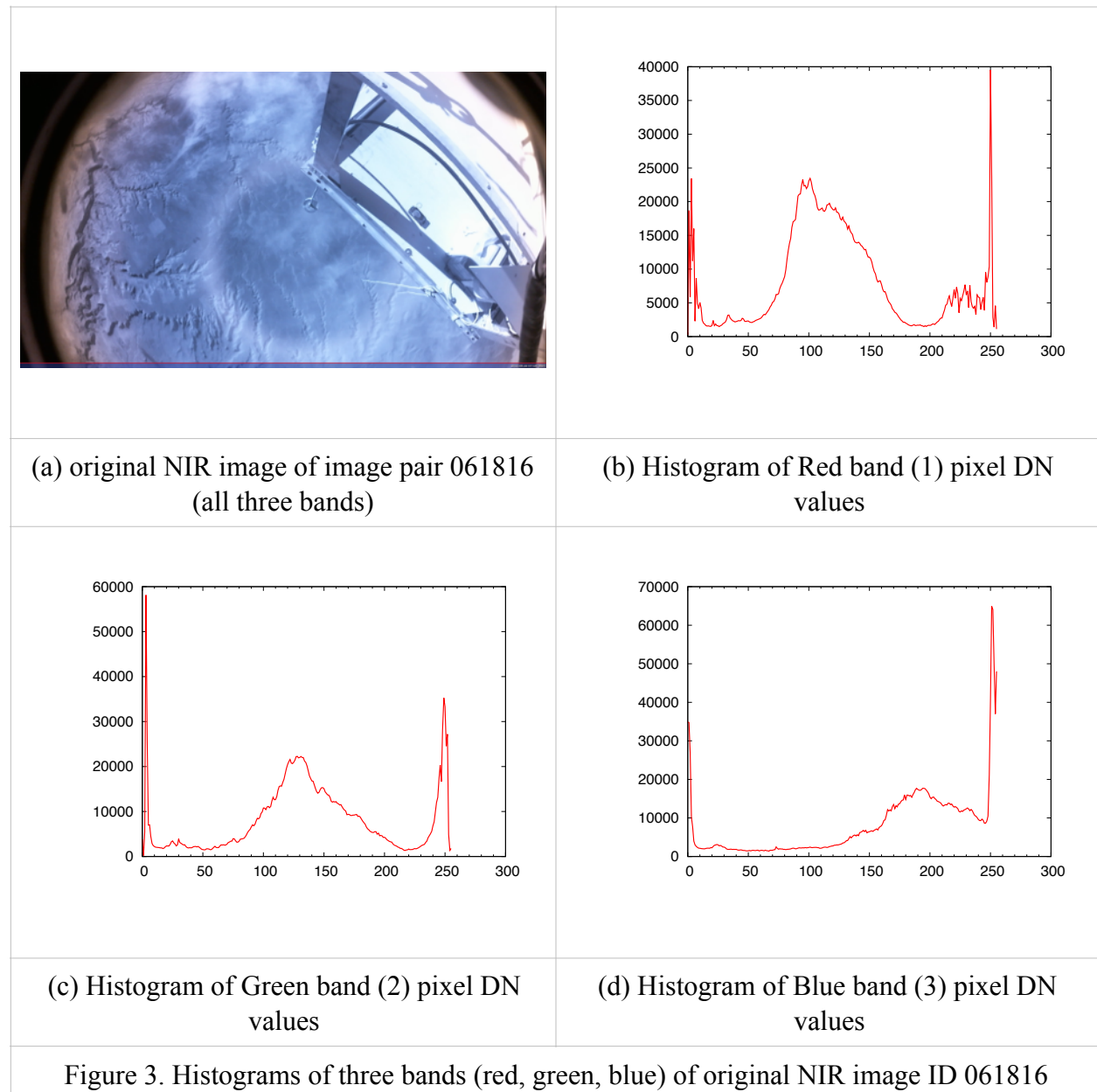



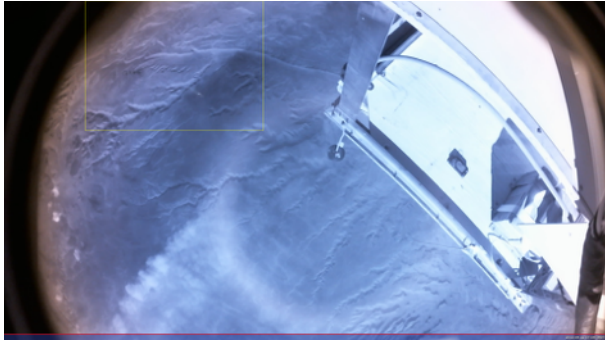
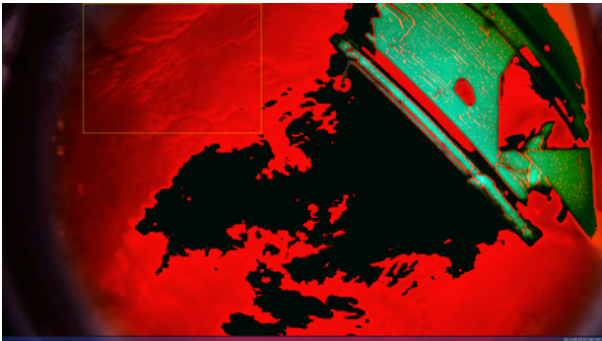
Figure 3 shows a NIR image of the same scene and three histograms which correspond to the red, green, and blue bands. Figure 3 (b) and (c) indicate that there are peak pixel populations

with DN values around 100 for the red and green bands, respectively. The blue band histogram, Figure 3 (d), shows a peak in DN values around 180. Each of the three bands has a second peak in DN values close to 255. Those pixels indicate the white parts of the NIR image which could be where there are clouds and the HASP gondola shown in Figure 3 (a).



### 3.3.1 Selection of regions of interest (ROI) within each image

In order to avoid processing the parts of an image pair where there was saturation in the red image, a region of interest (ROI) was selected from each image. Several steps were taken in this selection process. First, a script was developed to zero out saturated pixels in the red image. Every pixel in the red band of the red image with a DN value greater than 250 was set to 0 so they appear black. Such images are shown in part (c) of Figure 4. Note that parts of the image shown in Figure 4 (c) appear green because only the DN values in the red band of the image were set to zero, however the three band image is shown in Figure 4 (c).

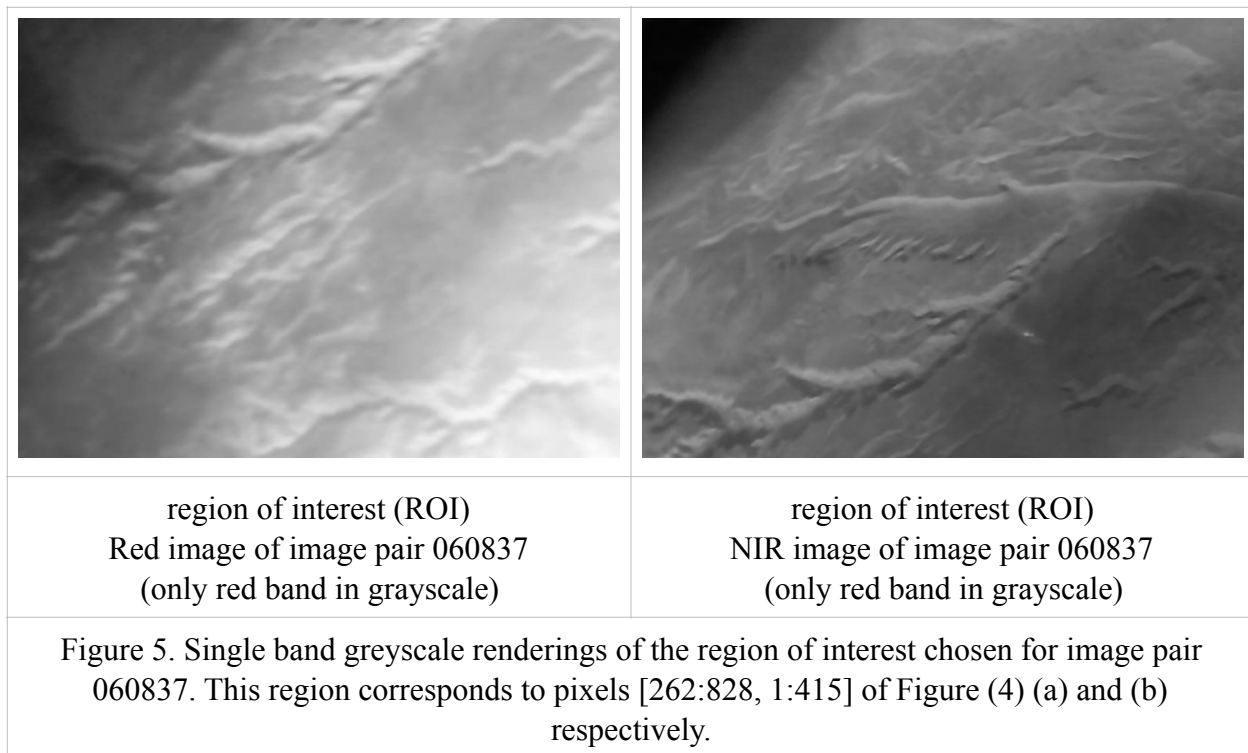
	
(a) original Red image of image pair 060837 (all three bands)	(b) original NIR image of image pair 060837 (all three bands)
	
(c) modified Red image of image pair 060837 with saturated pixels blacked out	
Figure 4. Zeroing out saturated reg pixels. (a) original red image, (b) original NIR image, (c) modified red image with pixels with DN values greater than 250 set to 0.	

The next step in the selection of a region of interest to avoid the saturated portions of the image was to display the red image with the blacked-out saturated zones. The red image was displayed in the ImageJ app. A rectangle was selected by hand to avoid the black zones and the (x,y) coordinates of the upper-left corner of the rectangle and its width and height were recorded.

Table 1 shows eighteen selected regions of interest for different image pairs. Each region of interest was chosen as a rectangular area of non-saturated pixels in the red image. The next step in the process was to extract only the red band of the red and NIR images of each pair and to choose the ROI within those images. Figure 5 shows the ROI of an example red and NIR image pair with ID 060837. This region corresponds to pixels [262:828, 1:415] of Figure (4) (a) and (b) respectively.

Table 1. Eighteen image pairs with image numbers and the pixel coordinates of the chosen region of interest for each.

Red image ID	NIR image ID	Processed	ROI x1:x2, y1:y2
060004	060001	NDVI, ROI	212:380, 1:667
060010	060007	NDVI, ROI	138:374, 1:681
060016	060013	NDVI, ROI	176:400, 1:693
060703	060701	NDVI, ROI	226:742, 1:533
060710	060707	NDVI, ROI	242:724, 1:527
060825	060822	NDVI, ROI	154:820, 1:445
060831	060828	NDVI, ROI	374:938, 8:316
060837	060833	NDVI, ROI	262:828, 1:415
060913	060910	NDVI, ROI	388:888, 28:258
060955	060952	NDVI, ROI	376:880, 10:246
061007	061004	NDVI, ROI	422:906, 24:252
061213	061211	NDVI, ROI	250:908, 1:151
061507	061504	NDVI, ROI	232:632, 520:1056
061725	061728	NDVI, ROI	136:264, 242:882
061819	061816	NDVI, ROI	248:528, 2:874
061825	061822	NDVI, ROI	226:490, 4:942
061831	061827	NDVI, ROI	226:552, 2:952
061837	061833	NDVI, ROI	238:540, 2:966



### 3.3.2 Calculation of NDVI for selected ROI

The normalized difference vegetation index (NDVI) was calculated for the region of interest in each image pair. As a first test, the NDVI calculation was performed on the raw DN values of the images. In this project, no attempt was made to correct for atmospheric factors such as air density or clouds. Furthermore, additional corrections should be made to evaluate reflectance values to achieve a standardized NDVI calculation. The calculated NDVI is based on the selected region of interest (ROI) in both red and NIR.

After the raw DN value approximations of NDVI-type calculation were performed, calculations with bandwidth correction were done. The red and near infrared filters are not the same bandwidth. Therefore the flux through them is unequal. To normalize the light flux through the band pass filters into each camera, the NIR images are multiplied by a bandwidth ratio of the Red filter bandwidth to the NIR filter bandwidth for NDVI processing. The specifications for the filters were as follows: the red filter (from Edmund optics) had a 650 nm center wavelength (CWL) with a bandwidth of 80 nm full-width half-maximum (FWHM), and NIR filter (also from

Edmund optics) with 850 nm CWL and 25 nm FWHM. Considering the bandwidth ratio of red to NIR, the bandwidth ratio of 3.2 was used.

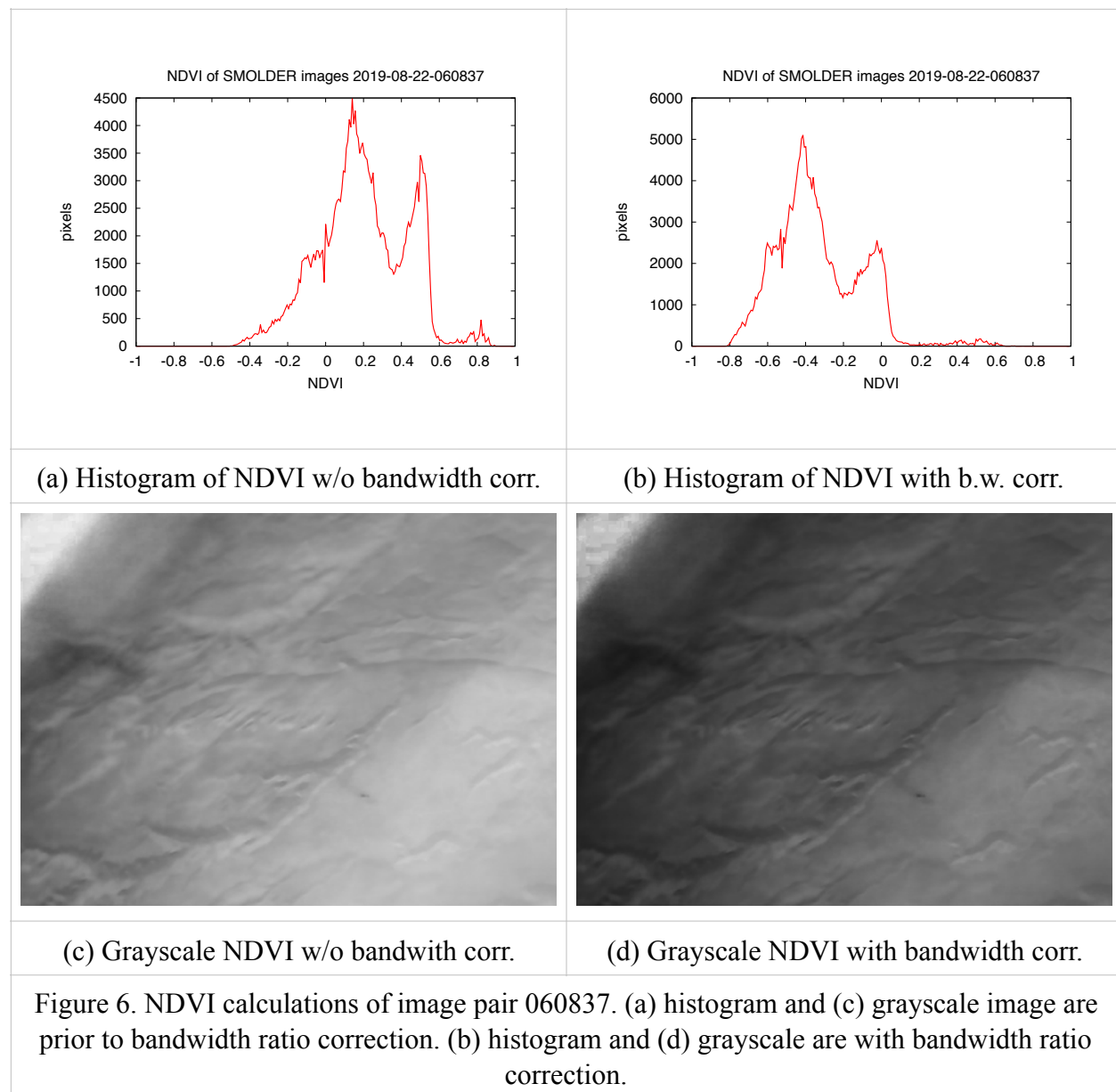
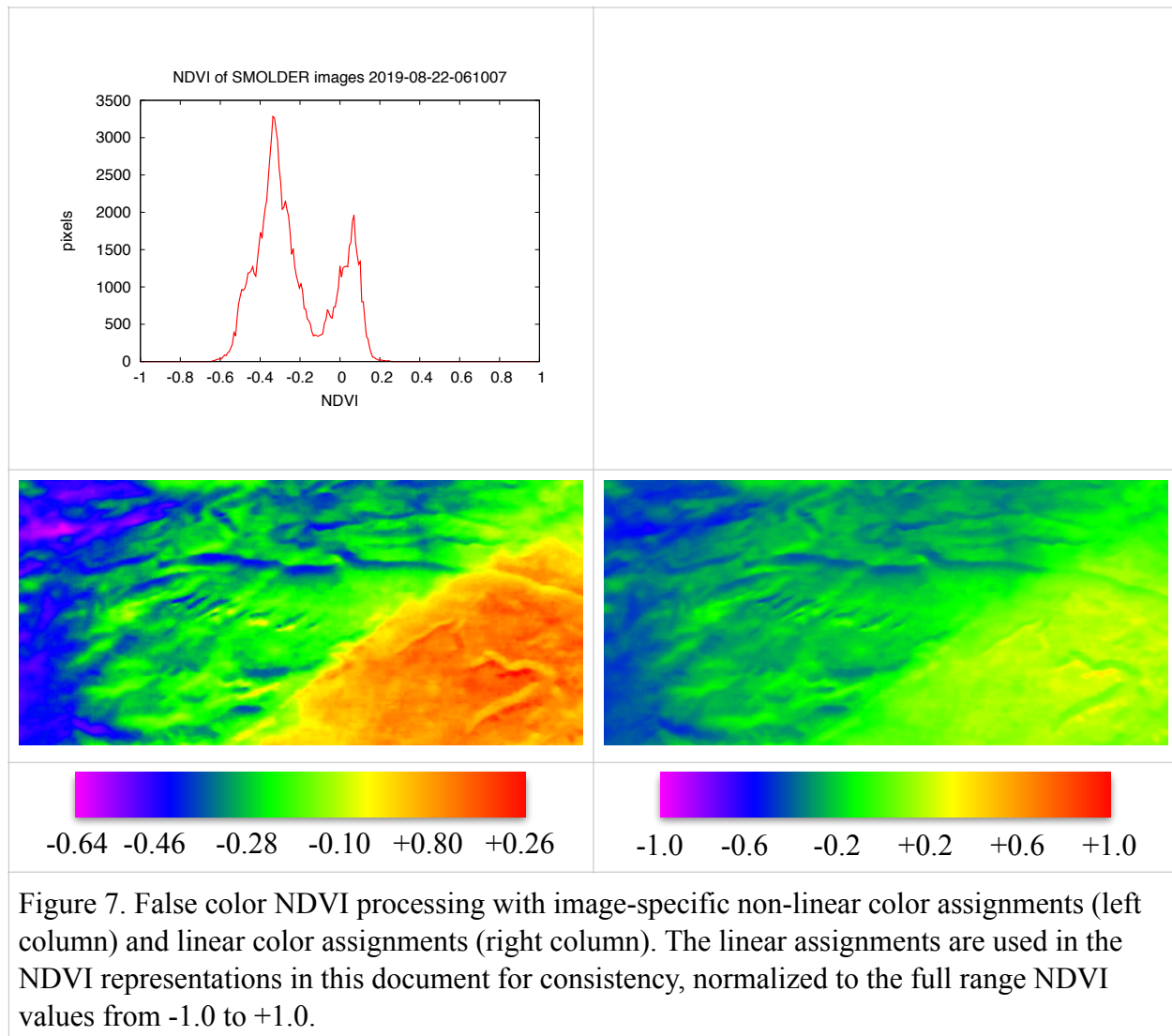


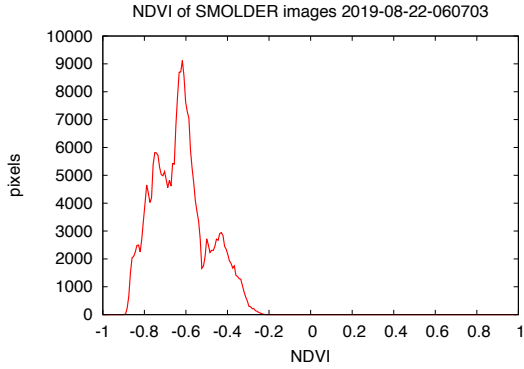
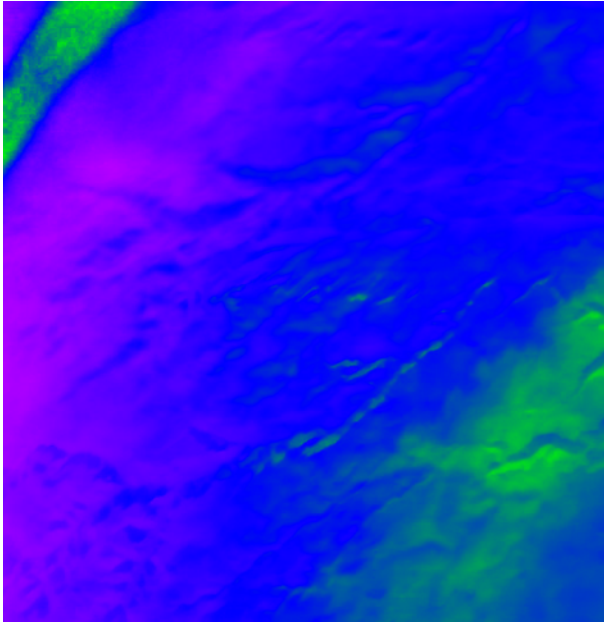
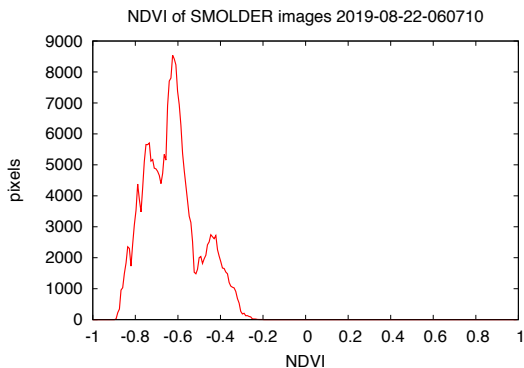
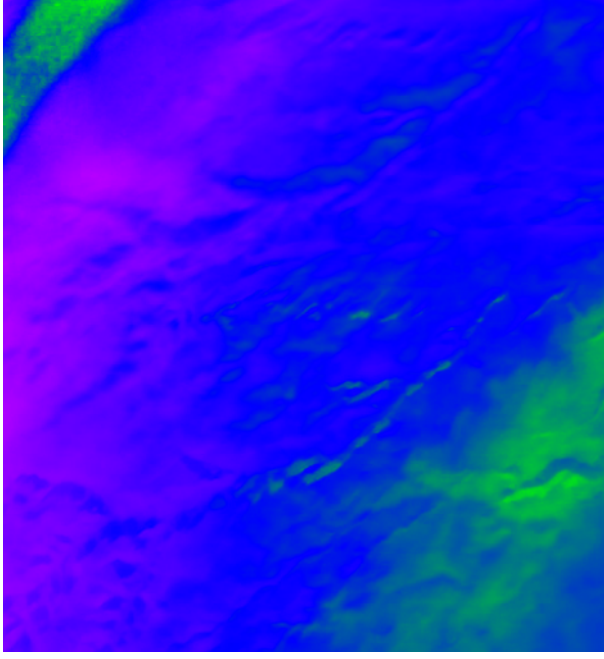
Figure 6 shows initial tests of NDVI without bandwidth correction and with bandwidth ratio correction. The bandwidth correction ratio was incorporated into all subsequent NDVI calculations.

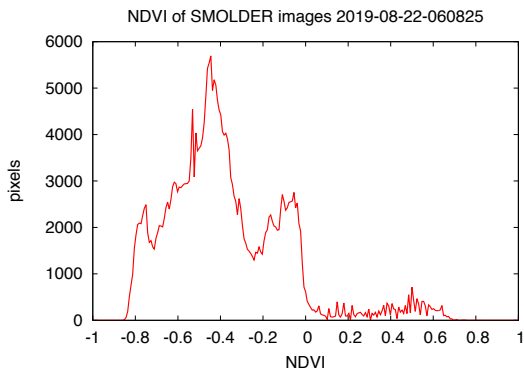
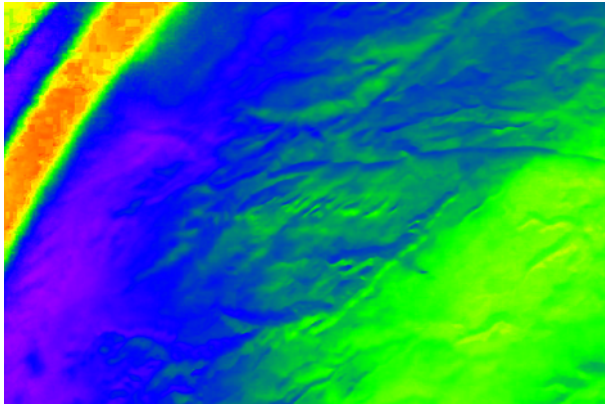
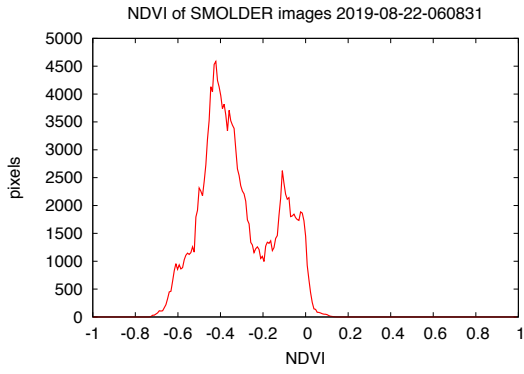
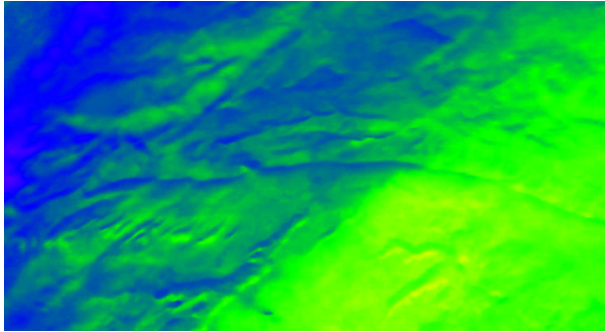
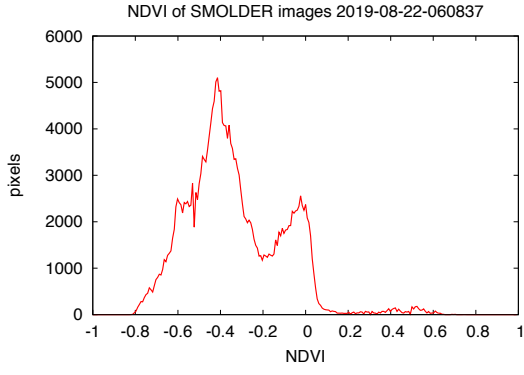
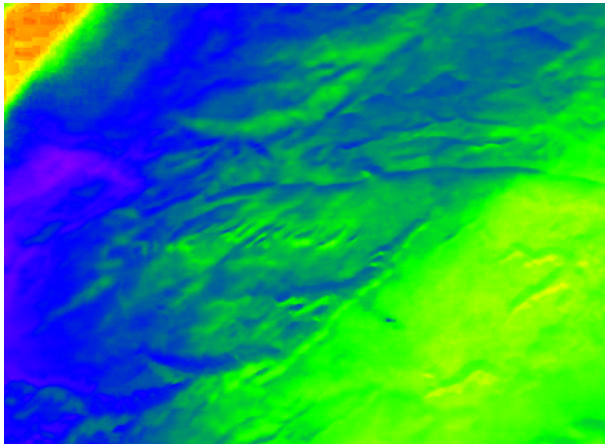
### 3.3.3 NDVI calculations for selected image pairs

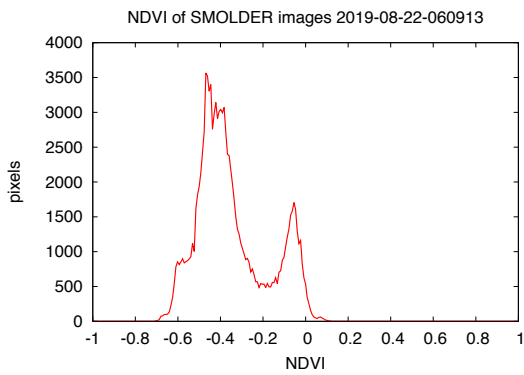
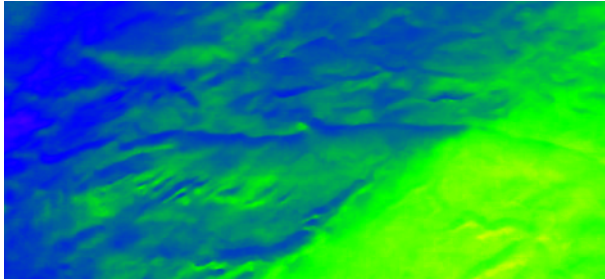
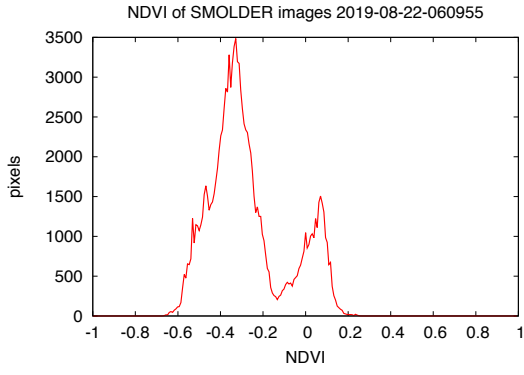
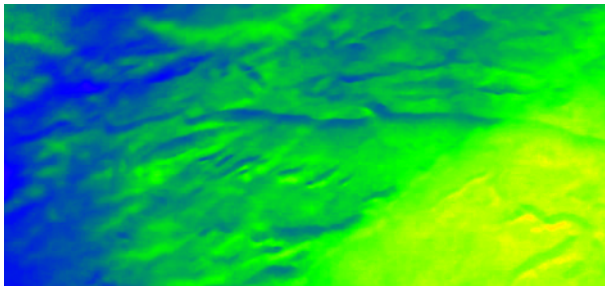
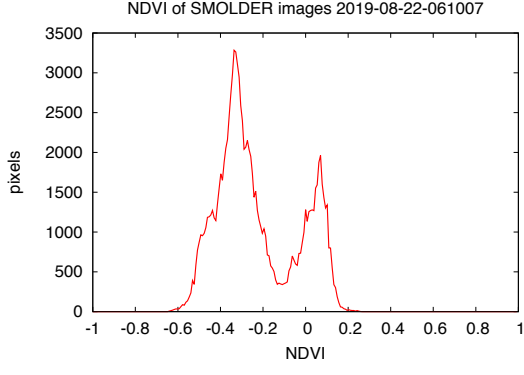
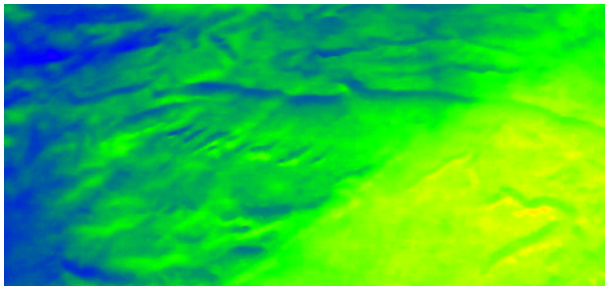
Fifteen image pairs were selected for NDVI processing for this report. The NDVI histogram and false color image for each of these 15 images pairs is shown in Figure 8.

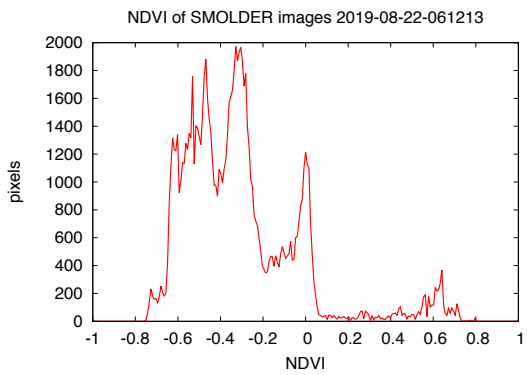
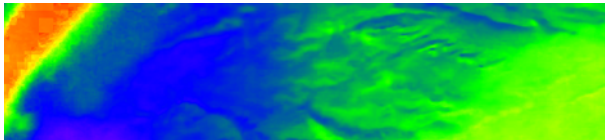
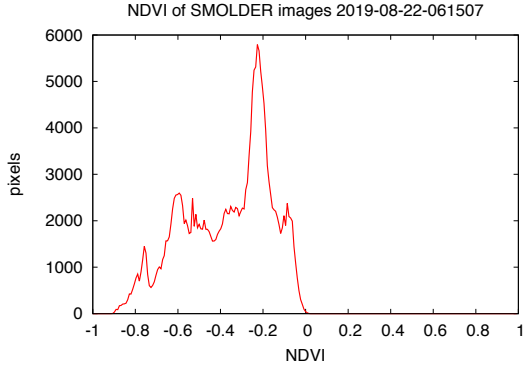
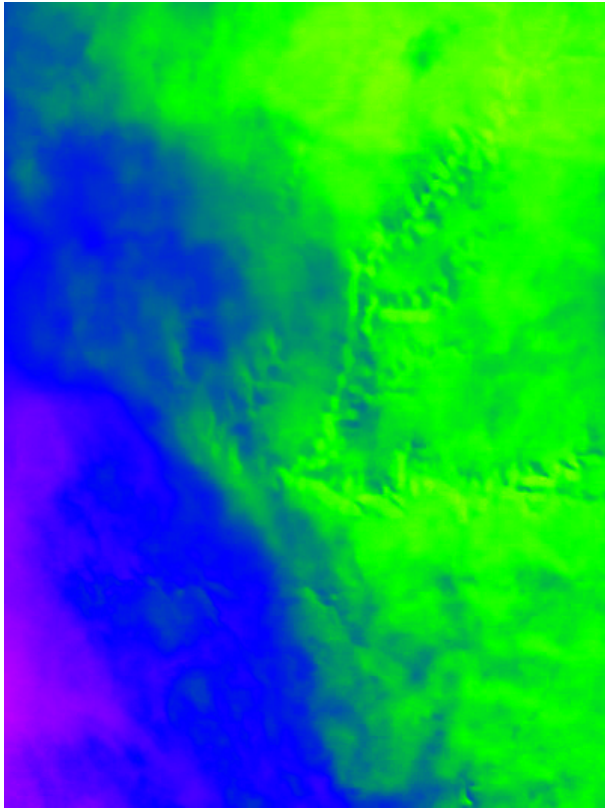


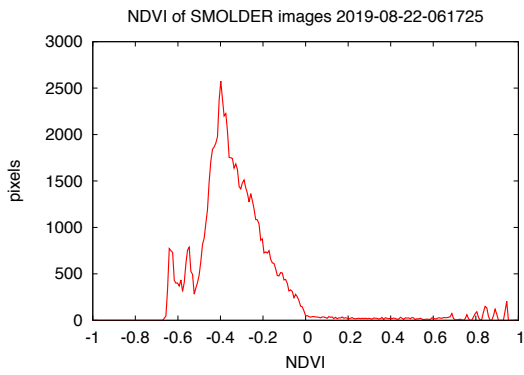
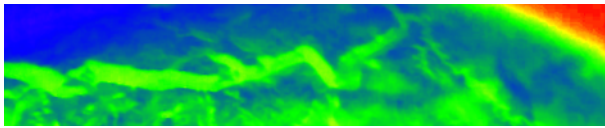
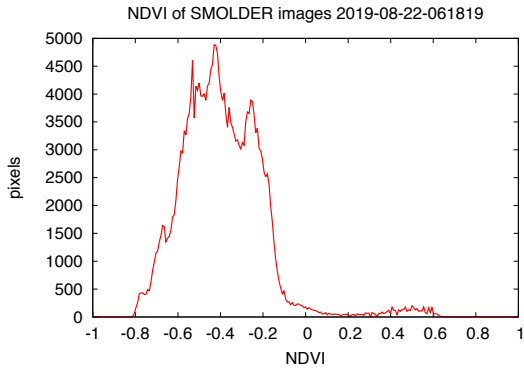
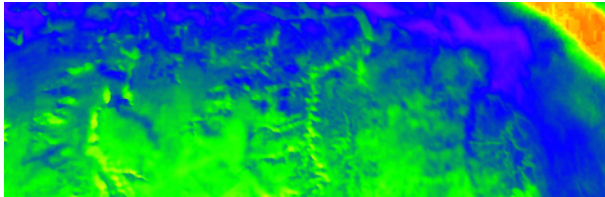
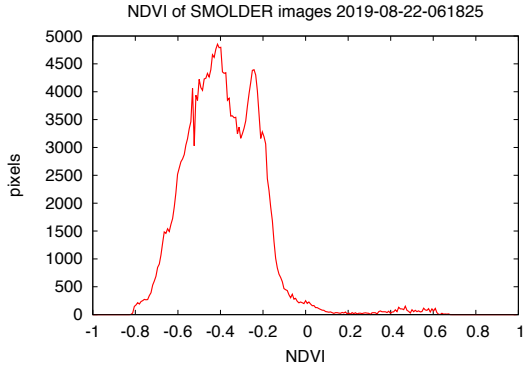
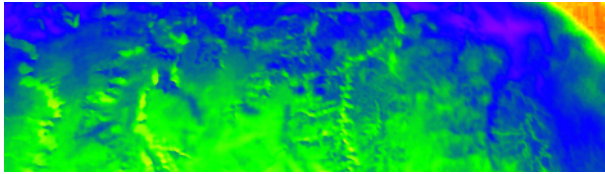


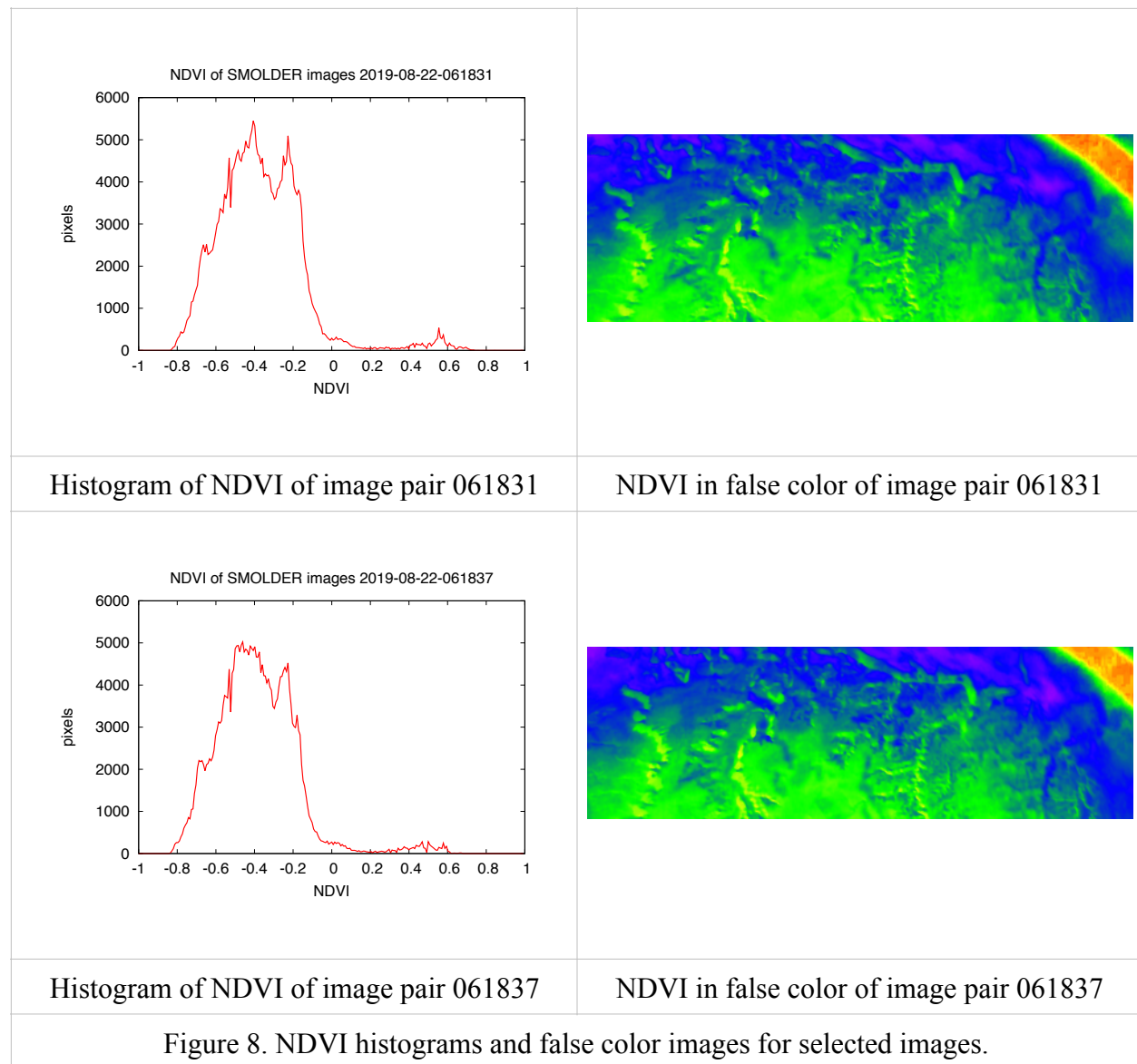
 <p>NDVI of SMOLDER images 2019-08-22-060703</p> <p>The histogram shows the distribution of NDVI values for image pair 060703. The x-axis represents NDVI values from -1 to 1, and the y-axis represents the number of pixels from 0 to 10,000. The distribution is bimodal, with a primary peak around -0.6 (approximately 9,000 pixels) and a secondary peak around -0.4 (approximately 3,000 pixels). The data is concentrated between -1.0 and -0.2.</p>	 <p>A false color NDVI image for image pair 060703. The image displays a landscape with varying vegetation density. High NDVI values (green) are concentrated in the upper left corner, while lower values (blue/purple) dominate the rest of the image.</p>
<p>Histogram of NDVI of image pair 060703</p>	<p>NDVI in false color of image pair 060703</p>
 <p>NDVI of SMOLDER images 2019-08-22-060710</p> <p>The histogram shows the distribution of NDVI values for image pair 060710. The x-axis represents NDVI values from -1 to 1, and the y-axis represents the number of pixels from 0 to 9,000. The distribution is bimodal, with a primary peak around -0.6 (approximately 8,500 pixels) and a secondary peak around -0.4 (approximately 2,500 pixels). The data is concentrated between -1.0 and -0.2.</p>	 <p>A false color NDVI image for image pair 060710. The image displays a landscape with varying vegetation density. High NDVI values (green) are concentrated in the upper left corner, while lower values (blue/purple) dominate the rest of the image.</p>
<p>Histogram of NDVI of image pair 060710</p>	<p>NDVI in false color of image pair 060710</p>

 <p>NDVI of SMOLDER images 2019-08-22-060825</p>	
Histogram of NDVI of image pair 060825	Grayscale NDVI of image pair 060825
 <p>NDVI of SMOLDER images 2019-08-22-060831</p>	
Histogram of NDVI of image pair 060831	Grayscale NDVI of image pair 060831
 <p>NDVI of SMOLDER images 2019-08-22-060837</p>	
Histogram of NDVI of image pair 060837	Grayscale NDVI of image pair 060837

 <p>NDVI of SMOLDER images 2019-08-22-060913</p>	
Histogram of NDVI of image pair 060913	NDVI in false color of image pair 060913
 <p>NDVI of SMOLDER images 2019-08-22-060955</p>	
Histogram of NDVI of image pair 060955	NDVI in false color of image pair 060955
 <p>NDVI of SMOLDER images 2019-08-22-061007</p>	
Histogram of NDVI of image pair 061007	NDVI in false color of image pair 061007

 <p>NDVI of SMOLDER images 2019-08-22-061213</p> <p>The histogram shows the distribution of NDVI values for image pair 061213. The x-axis represents NDVI values from -1 to 1, and the y-axis represents the number of pixels from 0 to 2000. The distribution is bimodal, with a primary peak around -0.4 (approx. 1900 pixels) and a secondary peak around 0.6 (approx. 400 pixels). There is a significant dip in pixel count between -0.2 and 0.0.</p>	 <p>A grayscale NDVI map for image pair 061213. The map shows a landscape with varying vegetation density. Darker areas (blue/purple) indicate lower NDVI values, while lighter areas (green/yellow) indicate higher NDVI values. The distribution of colors corresponds to the bimodal histogram shown in the adjacent panel.</p>
<p>Histogram of NDVI of image pair 061213</p>	<p>Grayscale NDVI of image pair 061213</p>
 <p>NDVI of SMOLDER images 2019-08-22-061507</p> <p>The histogram shows the distribution of NDVI values for image pair 061507. The x-axis represents NDVI values from -1 to 1, and the y-axis represents the number of pixels from 0 to 6000. The distribution is unimodal with a sharp peak around -0.2 (approx. 5800 pixels). There are smaller peaks around -0.7 and -0.5.</p>	 <p>A grayscale NDVI map for image pair 061507. The map shows a landscape with varying vegetation density. Darker areas (blue/purple) indicate lower NDVI values, while lighter areas (green/yellow) indicate higher NDVI values. The distribution of colors corresponds to the unimodal histogram shown in the adjacent panel.</p>
<p>Histogram of NDVI of image pair 061507</p>	<p>Grayscale NDVI of image pair 061507</p>

 <p>NDVI of SMOLDER images 2019-08-22-061725</p>	
Histogram of NDVI of image pair 061725	Grayscale NDVI of image pair 061725
 <p>NDVI of SMOLDER images 2019-08-22-061819</p>	
Histogram of NDVI of image pair 061819	Grayscale NDVI of image pair 061819
 <p>NDVI of SMOLDER images 2019-08-22-061825</p>	
Histogram of NDVI of image pair 061825	NDVI in false color of image pair 061825



## 4 Discussion

As can be seen in Figure 8, the NDVI values computed from the images collected in this project range from -0.8 to 0 while a few regions have some positive NDVI values as high as +0.2. Most of the histograms have a peak NDVI value of -0.4. It is interesting to note that some of the images show a bimodal distribution of NDVI values, which can also be inferred from the false color images which are predominantly blue and green. It is important to note that the red-orange strip at the corner of some of the images is an artifact of the edge of the camera lens, and does

not represent a positive NDVI value. The negative NDVI values indicate that the intensity of the NIR reflectivity is less than that of the red band, which is indicative that the terrain is devoid of green plants. This agrees with visible terrain that can be seen in the Google maps flight path which is shown in figure 9. It can be seen that the HASP Calculation of true NDVI requires calibration with exposure times and calibration of the wavelength response of the camera sensors. Atmospheric correction also plays an important role in the computation of standard NDVI values. However, it is important to note that raw DN values are being used to compute the NDVI in this study.

#### **4.1 DN values and Saturation**

The original red and NIR images were taken using standard high definition web cameras. Each image has 1920 by 1080 pixels, commonly known as a two megapixel image. These webcams take RGB images, which means that each pixel has three color components, namely red (R), green (G), and blue (B). When the payload code saves each image to a file, the format used has eight bits per color band per pixel. This means that each of the R, G, and B color bands can have a value of 0 to 255. A pixel value is sometimes referred to as a digital number, or DN. Thus, the red band of an image could have a DN value of 255 which would be pure red. In RGB images the red component is band 1, the green component is band 2, and the blue component is band 3. For an RGB image, the value of 255, 0, 0 would indicate 255 red, 0 green, and 0 blue which is also red.

One problem with digital cameras and remote sensing systems is overexposure. When the charge-coupled device (CCD) sensors take in too much light during the exposure time for an image, the sensor is saturated and the maximum DN value is recorded in the image. When analyzing an image, one cannot distinguish between a normal DN value of 255 and an overexposed saturated value. Including saturated pixel values in image analysis will result in unreliable data and misleading results.



Figure 2 (a) shows the original Red image of image pair 061819. Again, this is a 2 megapixel RGB image. As seen in the histogram in Figure 2(b), there are more than 450,000 pixels with a band 1 (red) DN value of 255 and significant numbers of additional pixels with DN values also above 250. That amounts to more than 20% of the image. That means that a significant part of the image was saturated in the red band. There were a similar number of pixels with DN values close to zero in the green and blue bands as indicated in Figure 2 (c) and (d). This indicates that the red filter was highly effective, with only a small amount of green and blue wavelengths passing through the filter. Almost all of the red images include significant portions that are saturated. Since most of the red-filter images were saturated, the saturated red pixels were eliminated by setting DN values above 250 in the red band to 0. From the resultant image, a region of interest was selected and matched with a corresponding NIR image and the NDVI values were computed.

#### 4.2 False Color for NDVI

NDVI is given by the equation  $NDVI = \frac{NIR - red}{NIR + red}$ . For any given pixel of the original red and

NIR images, the resultant pixel of NDVI will have a value in the range -1.0 to +1.0. When NDVI images are displayed these values must be transformed into a form that can visibly represent the NDVI. There are two forms of visible rendering of NDVI shown in this study: grayscale and false color. For grayscale, a simple linear scaling to display pixels was used.

Figure 6 (a) shows the non-bandwidth-corrected histogram of NDVI values of image pair ID 060837 with peaks around +0.15 and +0.5, whereas the bandwidth corrected histogram in (b) has shifted to lower values with peaks around -0.4 and  $\pm 0.0$  and the shape of the curve altered by the correction. Accordingly, the Figure 6 (c) non-bandwidth correction grayscale NDVI image is rather light whereas the Figure 6 (d) bandwidth corrected grayscale NDVI image is much darker due to those lower NDVI values.

To calculate false color NDVI values, the `davinci colorize` function was used [5]. This assigns six colors to different NDVI values. By default, this function uses the distribution of



actual values in the NDVI image which will result in a non-linear stretch of the NDVI values so that it uses all six colors, thus the colors have different meanings in each image. Instead, a linear assignment of the six colors to six specific NDVI values was given to the `colorize` function. The values assigned are violet = -1.0, blue = -0.6, green = -0.2, yellow = +0.2, orange = +0.6, and red = +1.0. Figure 8 shows both the non-linear image-specific false color NDVI for image ID 061007, and the normalized linear NDVI. All remaining false color NDVI images in this document use the normalized scale.

## 5 Conclusions

### 5.1 Summary

The Team SMOLDER payload was successfully launched onboard the HASP balloon mission from Fort Sumner, New Mexico on September 5, 2019. HASP traveled 378 miles at an altitude of 36 km over a period of 7 hours and landed near the southeastern corner of Utah. The two webcams on the SMOLDER payload successfully captured in excess of 4,000 images during this flight. The payload was successfully retrieved by one of the team members and returned to ASU. The SD card from the payload's Raspberry Pi controller was retrieved and the images were copied for offline analysis.

The images captured by webcam A with the red filter were mostly saturated due to the autoexposure settings in the webcam driver. The images were processed by excluding the saturated pixels and correlating to the corresponding portions of the near IR images from webcam B. Uncalibrated NDVI values were computed using `davinci` software. Limitations of the autoexposure settings used by the webcam driver prevented the calibration of the wavelength response of each of the webcams with their respective filters.

The NDVI values generally range from -0.8 to 0.0, indicating that the terrain along the flight path does not contain detectable vegetation. This lack of vegetation correlates with the terrain along the flight path in Google Maps. Vegetation indices are most responsive and effective with areas of dense vegetation. The project was a success because it yielded realistic, although uncalibrated, NDVI values which are consistent with the surveyed terrain[6].

## 5.2 Lessons Learned

Our team learned several lessons during the course of this project. These include the following: Color cameras are not suitable for use with bandwidth filters because although the filter is only letting in red light or near infrared light, this light is being recorded by three different color sensors. These color sensors are designed to adjust autoexposure to achieve white balance. Therefore if the light for only one color is being allowed by the filter, then the RGB sensors are waiting for white balance, so the camera overexposes the image. Therefore autoexposure is also not suitable for multi-band studies. Webcams do not capture images in the RAW format. Data was recorded in a compressed JPEG format. Having two Raspberry Pis, one to control each camera, would have made it possible to record images simultaneously, ensuring that the same area is being recorded in both bands.

For follow-up missions involving multispectral remote sensing, we would recommend using monochromatic cameras that allow for manual control of exposure times. Measurement of sensor response to each wavelength with various exposure times can then be used to optimize the exposure time with each filter. Having two separate Raspberry Pis to ensure simultaneous image capture would also improve accuracy. Also recording GPS data for each image and having an accurate timestamp would help in the geolocation of the images.

In conclusion, this SMOLDER HASP mission was a success in demonstrating that multispectral remote sensing images can be obtained by a HASP payload and these images can be used to calculate vegetation indices. Furthermore, this mission was a success because the team members learned numerous technical, computational and organizational skills during the course of this project.

## **Acknowledgements**

We are grateful to our faculty advisor, Prof. Chris Groppi for his inspiring guidance, encouragement, and support. We would like to thank our faculty mentor Dr. Ernest Cisneros for advice and Prof. Paul Scowen and Prof. Phil Christensen for their suggestions about image analysis. We would also like to thank Marko Neric and Logan Jensen for assistance with testing and calibration of the cameras and Alexa Drew for outreach and fundraising. Furthermore, we would like to thank Dr. Guzik and Dr. Granger for leading and organizing the 2019 HASP project and for their encouragement and support throughout the year.

## **References Cited**

1. Earth Observatory. Remote Sensing. EOS Project Science Office. NASA Goddard Space Flight Center. ([earthobservatory.nasa.gov](http://earthobservatory.nasa.gov)).
2. Qi, Jianguo & Chehbouni, A & Huete, Alfredo & Kerr, Y.H. & Sorooshian, Soroosh. (1994). A Modified Soil Adjusted Vegetation Index. *Remote Sensing of Environment*. 48. 119-126.
3. USGS. Landsat 7 Thematic Mapper Band Designations. Landsat Missions. United States Geological Survey. U. S. Department of the Interior.
4. Weier, John & Herring, David. (2000). Measuring Vegetation (NDVI & EVI). NASA Earth Observatory. NASA Goddard Space Flight Center. 30 Aug. 2000.
5. Arizona State University. davinci wiki. (<http://davinci.asu.edu>) Web.
6. HASP (2019). High Altitude Student Platform. Louisiana State University Department of Physics and Astronomy, Space Sciences Group. (<https://laspaces.lsu.edu/hasp/>)

### Team SMOLDER: Roles and Demographics

Name	Role	Start Date	End Date	Education	Gender	Ethnicity	Race	Dis-ability
Paras Angell	Science and Data Analysis Lead	August 2018	December 2019	Undergrad	Male	Non-Hispanic	Asian-Caucasian	Yes
Megan Bromley	Testing Officer	August 2018	May 2019	Undergrad	Female	Non-Hispanic	Caucasian	
Henry Cardamone	Mechanical Lead	August 2018	May 2019	Graduate	Male	Non-Hispanic	Caucasian	No
David Lewis	Filter Subsystems Lead	August 2018	September 2019	Undergrad	Male	Hispanic	Hispanic	No
Tim McMillen	Electrical Lead Team Lead (Summer 2019)	August 2018	September 2019	Undergrad	Male	Non-Hispanic	Caucasian	Yes
Michael Oals	Software Engineer	August 2018	September 2019	Undergrad	Male	Non-Hispanic	Caucasian	No
Jenna Robinson	Systems Engineer Original Team Lead	August 2018	May 2019	Grad Student	Female	Non-Hispanic	Caucasian	No
Chris Groppi	Faculty Advisor	August 2018	December 2019	Professor	Male	Non-Hispanic	Caucasian	No
Marko Neric	Graduate TA	January 2019	May 2019	Grad Student	Male	Non-Hispanic	Caucasian	No
Logan Jensen	Calibration Consultant	May 2019	November 2019	Grad Student	Male	Non-Hispanic	Caucasian	No
Paul Scowen	Faculty Mentor	August 2018	May 2019	Professor	Male	Non-Hispanic	Caucasian	No
Ernest Cisneros	Faculty Mentor	August 2018	December 2019	Professor	Male	Hispanic	Hispanic	No
Hema Werner	Volunteer	July 2019	September 2019	Grad Student	Female	Non-Hispanic	Asian	No
Brad Werner	Volunteer	July 2019	September 2019		Male	Non-Hispanic	Caucasian	No

**Team SMOLDER Graduation Information**

Name	Graduation Date	Degree	Current Status
Paras Angell	December 2019	B.S. Earth and Space Exploration (Geology)	Undergraduate Student
Megan Bromley	December 2019	B.S. Astrobiology	Undergraduate Student
Henry Cardamone	May 2019	B.S. Astrobiology	Information not available
David Lewis	December 2019	B.S. Astrobiology	Undergraduate Student
Timothy McMillen	May 2020	B.S. Astrophysics	Undergraduate Student
Michael Oals	December 2019	B.S. Astrobiology	Undergraduate Student
Jenna Robinson	May 2019	B.S. Astrobiology	Graduate Student

## Appendix A

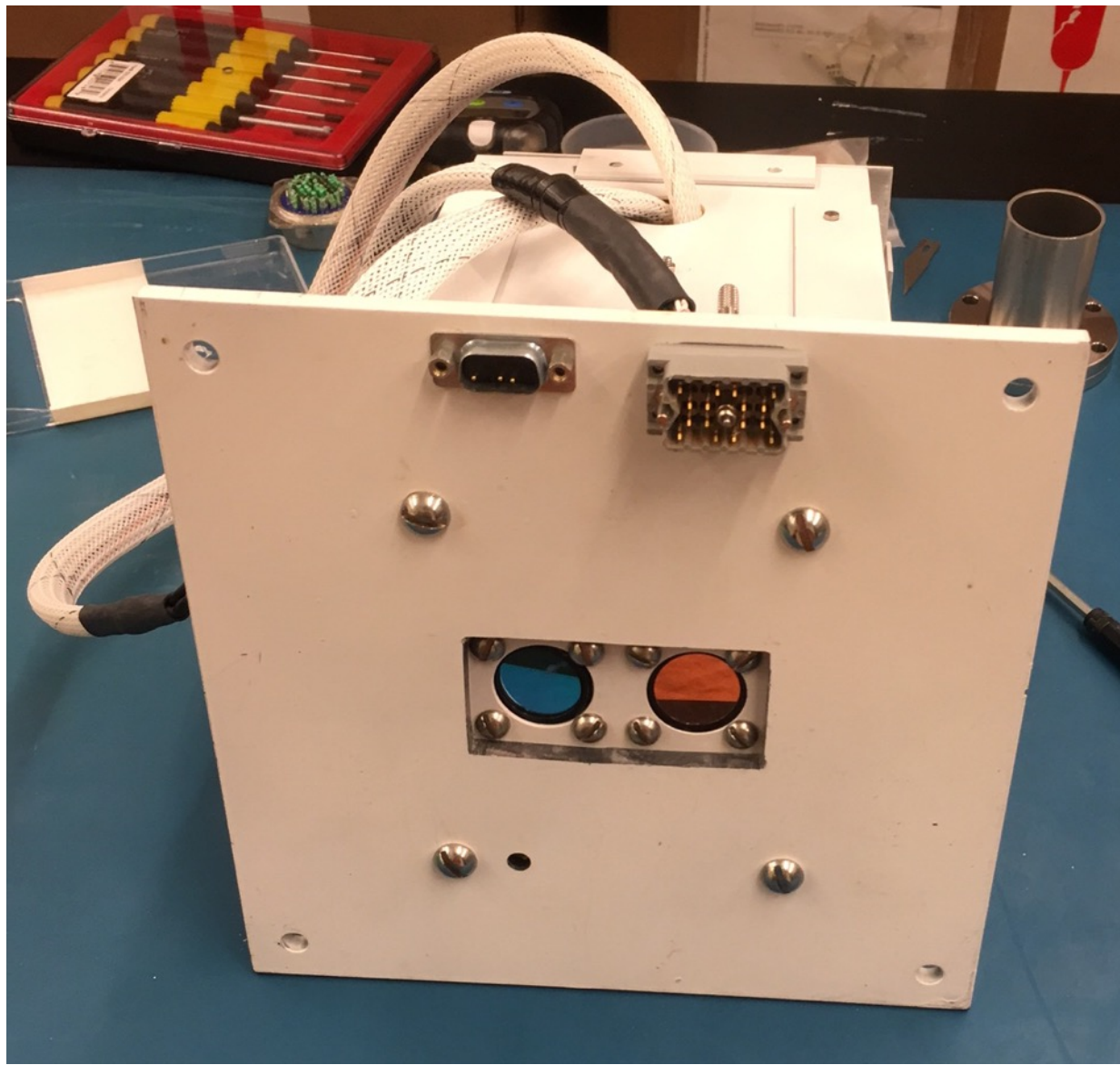


Figure A1. Photograph of SMOLDER payload for HASP 2019 mission.

## Appendix B



Figure B1. HASP 2019 mission flight path from Google Maps. (<https://laspace.lsu.edu/hasp/>)